Petrographical and Diagenesis Characterestics of Benavi Ironstone in Kurdistan Region-Northern Iraq

Ali Taha Yassin[*] and Mudhafar M. Mahmoud[**]

[*] **Assistant Chief Geologist, Iraq Geological Survey, P.O. Box 986, Alwiya, Baghdad, Iraq, e-mail: alitahayassin@geosurviraq.com , alitahayassin@yahoo.com**

[**] **University of Baghdad, College of Science, Earth Sciences Department, retired, Iraq**

Abstract:

Benavi Ironstone (BI) is hosted in highly fractured carbonate beds of Hadiena Formation and located about 20 kilometers N-NW of Amadiya District in Duhok Governorate – Kurdistan Region north of Iraq. The outcrop of BI extends about 2 kilometers with thickness up to 13 meters and occurs within Jurassic – Cretaceous sequence. Forty eight samples were collected from ten sections that represent this elongated body. Petrographical study under transmitted and reflected light microscopy showed that BI is related to algal-bioclastic-packstone host rocks; this facies suffered from many diagenetic processes such as iron oxides replacement, neomorphism, pyritization, dolomitization, silicification and phosphatization. Depending upon iron rich sediments textural classification, BI was also classified as iron-packstone. Iron oxides have replaced partially and completely the calcareous structures, consequently, deposits with unusual iron oxides contents, were produced. Pyrite is unevenly distributed throughout this body, which occurs in two patterns: euhedral massive and framboidal forms. Euhedral magnetite crystals are also present. Chamosite was mostly observed around impregnation fossils by iron oxides.

Keywords: ironstone, Iraq, Kurdistan, Benavi, iron-packstone

Introduction

Sedimentary iron ores can broadly be considered as occurring in three major classes: bog iron ores, ironstones and banded iron formations (Craig and Vaughan, 1981). Banded iron formations belong to Precambrian age, whereas ironstones to phanerozoic age (Pettijhon, 1975). Phanarozoic sedimentary ironstones are usually thin sequences which were deposited in shallow marine or non- marine environments (Young and Taylor, 1989). Practically, iron is present in all sedimentary rocks to the extent of few percent but less commonly it forms ironstones and iron formations where the iron content exceeds 15% (James, 1966). The behavior of iron and precipitation of its minerals are strongly controlled by the chemistry of the surface or diagenetic environment (Tucker, 1981). The deposits and occurrences of iron ores in Iraq are located in the mountain folded zone of the country (Asnawa, Mishau, Benavi…) and in the platform area western desert (Gaara and Hussainiyat), (Etabi, 1982). Benavi Ironstone (BI) is one of these occurrences which is an elongated E-W body hosted in ferruginous-carbonaceous breccias horizon occurring in Jurassic-Cretaceous sequences (Chaikin, 1970). Initially, this ore body was believed to be sedimentary iron ore deposit related to shallow- marine high - energy in origin (Geozavod, 1981). It has been found that applied studies covering Benavi area were very limited; no bore-holes were drilled to investigate

the extensions of BI. However, occurrences of sedimentary iron ores near Benavi and Hadiena villages are mentioned by:

1-Wetzel (1950) showed that Hadiena formation consists of angular fragments of hematite in matrix of ferruginous limestone in the type locality south of Hadiena in Amadia district, northern Iraq.

2-Mc Carthy (1955) described BI as a ferruginous grit horizon,(5-6 m thick) extending for more than (1 km) and occurs in the Chia Gara series of Hadiena and Benavi villages.

3-Boukhtoyarov and Yevlentyev (1962) described the horizon as hematitic sandstones (6 m) in thickness.

4-Chaikin (1970) subdivided BI to three beds: A-Basal portion consists of dark gray limestone with clear fragmental texture; the ferruginization is represented by dispersed goethite and ovoids of hematite were recorded especially at its uppermost part. B- Intermediate part which consists of hematitic carbonate rocks with reddish-lilac in appearance consisting of oval or rounded fragmentas and groundmass (about 2.4-4 m thick), ovoids of hematite are most common than the previous part. C-The uppermost part of the ore – bearing horizon with (5-6 m) thick characterized by grey sandy limestone and brown siliceous hematite fragments.

5-Geozavod (1981) mentioned that a series of detrital ferruginous limestones with notable iron concentrations in the form of limonite, goethite or hematite lies in the Upper Cretaceous deposit of Hadiena formation between the villages of Benavi and Hadiena which is about (25m) thick.

6-The mineralogical criteria of this deposit were studied carefully by modern techniques (Yassin and Mahmoud, 2012), they showed that that BI composed of mineral assemblages: carbonates (calcite, siderite, ankerite), iron oxides/hydroxides (hematite, goethite, limonite, magnetite), sulphides (pyrite, arsenopyrite), silicates (kaolinite, chamosite, glauconite, quartz) and apatite. Calcite is the main mineral in BI which is mostly impure containing Mg^{+2} and Fe^{+2}. Siderite and ankerite are minor.

7-Yassin, 2009 mentioned that the geochemical analyses of Fe_2O_3 ranges (3.28-33.9%) with an average of (20.44%), which is considered as low-grade ironstones and he interpreted the very strong negative correlation between CaO and Fe_2O_3 to the replacement of calcareous components by iron minerals suggesting epigenetic ores formd by the diagenetic replacements of carbonate rocks; and he attributed the negative correlations of CaO with SiO_2, Al_2O_3, P_2O_5, Co, Ni and Zn to the high effect of diagenetic processes, he also classified this iron rich body as Phanerozoic ironstone based on chemical anlyses (Yassin, 2009). This research aimed to clarify the petrographical characterstics of BI to understand the textural relationship between its constituents to throw some light on their genesis.

Location

BI lies about 1 Km (S-SW) of the Benavi village which is about (19-20) km (N-NW) of Amadia district in Duhok governorate - northern Iraq figure 1.

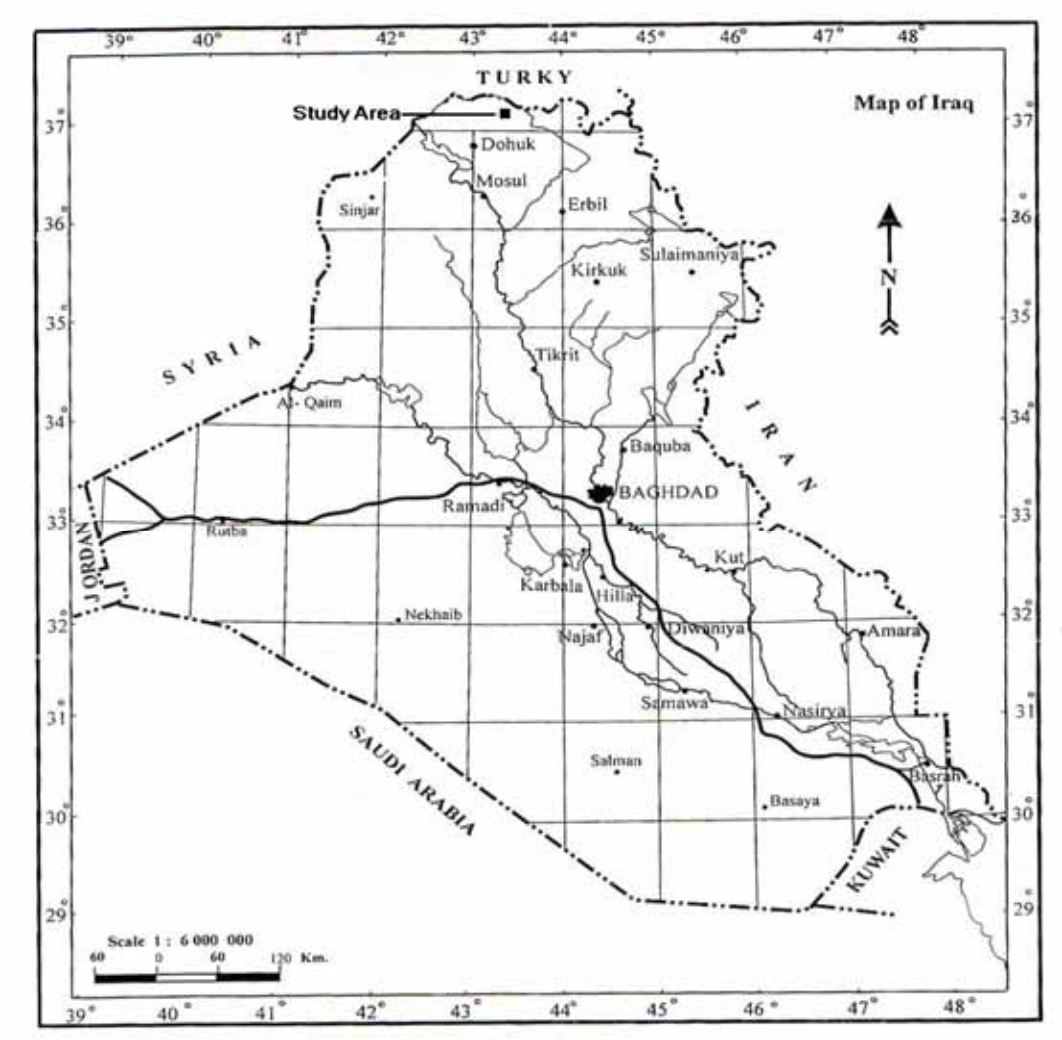

Figure 1: Location map of Benavi Ironstone (BI).

Geological and Tectonic Settings

BI is located in Northern Ora Thrust Zone of Iraq, figure 2, (Jassim & Goff, 2006). The structural pattern in this zone is characterized by a relatively long, east-west trending anticlinorium with three dome shaped where the oldest Paleozoic rocks are cropping out. The southern limbs of the anticlinorium are the steeper ones. The northern flanks are less disrupted faults, the southern steeper flanks where the Jurassic – Cretaceous beds are concentrated and accompanied by conspicuous thrust fault (Buday and Jassim, 1987). It is believed that BI belongs to Hadiena Formation, this formation was first defined by Wetzel in 1950 from the Hadiena area of the northern thrust zone, to the north west of Amadia district. The Hadiena formation consists of three divisions. The uppermost being the most typical one, the lower division consists of dolomitized limestone with vestiges of conglomeratic and fragmental elements. The middle division is composed of silty detrital calcareous marls and marly sandy limestone containing detrital hematitic, phosphatic and chert grains and the upper division, which is composed of conglomeratic and fragmental limestone consisting of angular fragments of hematite in matrix of ferruginous limestone (Buday, 1980).

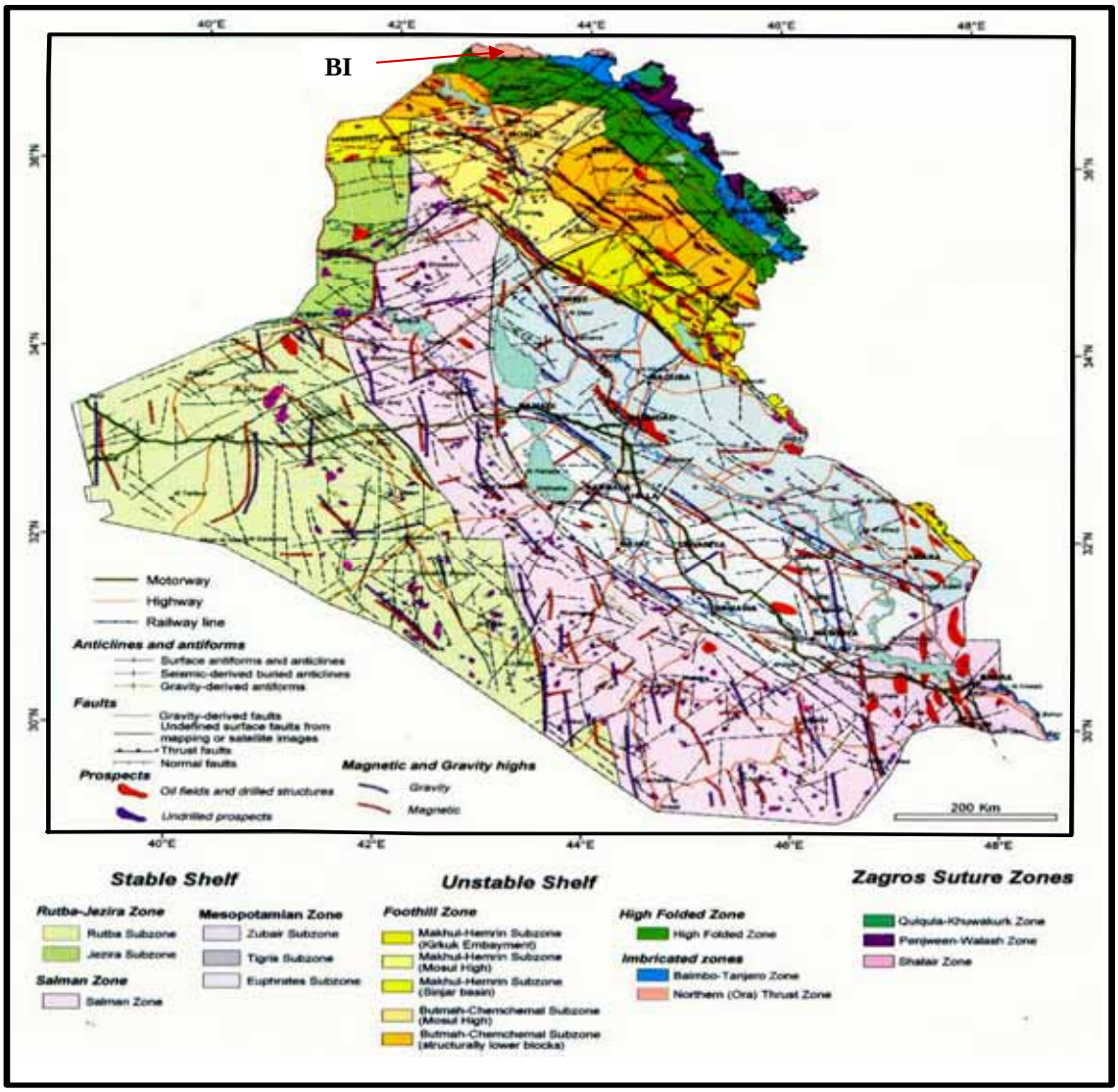

Figure 2: Tectonic Map of Iraq (after Jassim & Goff, 2006), shows location of Benavi Ironstone (BI) within Northern Ora Thrust Zone of Iraq.

Methodology

Eighty of thin sections for (48) samples were prepared for petrographic examinations under transmitted light microscopy. Some samples have been cut in two directions perpendicular to each other. Fifty eight of them were treated with Alizarin red solution to distinguish between calcite and dolomite according to (Friedman, 1959; Dickson, 1965), in this test, the color of calcite turned red-brown, whereas dolomite was not affected. Forty polished sections were made and studied under reflected light microscopy at the Laboratories of GEOSURV-Iraq. Some samples have been investigated under Scanning Electron Microscopy at Ecole-De Mines –Ales in France.

Petrography

The main petrogaphical constituents in BI are allochems and spary calcite cement. The allochems composed of high amount of skeletal components including calcareous red algae and other bioclasts with very small amounts of non-skeletal components (lithoclasts, detritul minerals

and clay). Calcareous red algae are very common in all BI samples; they have skeletons composed of cryptocrystalline calcite (Tucker, 1981).

Their size are measured with a range (0.11-1.68 mm), and regular cellular structure is present (Plate 1-A). Bioclasts is less common compared with red algae including echinoderms, shell fragments with few amount of foraminifera. Echinoderms acts optically as a single crystal of calcite, consequently each element uniformly extinct under crossed nicoles in a polarizing microscope. The uniform optical reaction of these skeleton elements is caused by the parallel arrangement of the c-axes of the calcite crystals which constitute the skeletal elements (Plate 1-B and C), (Flugel, 1982). Most of the studied samples contain echinoderms, their sizes range between 0.3 mm to 1.4 mm in diameter. Shell fragments are less common, in comparison with echinoderms that range in size between 0.36 mm to 0.78 mm (Plate 1-D). Foraminifera are observed in some samples and biserial type is more common than other foraminifera species (Plate 1-E). Sponge specules is also observed in some samples (Plate 1-F).The groundmass of the studied samples is mainly composed of spary calcite.

Classification

In this study, we adopted the definition of "microfacies" after Flugel (1982) which is most widely used as it is based on the simplest textural classification (the particle fabric and the kind of particle binding during sedimentation). This textural classification is the first step to identify the lithofacies of the studied samples aiming at recognizing their original depositional environment. According to this classification, limestones are divided in to three main textural groups: mud - supported (mudstone and wackstone), grain-supported (packstone and grainstone) and biologically bound during deposition (boundstone). Mudstones and wackstones contain less than 10 % grains; mud is still present in packstone which are grain-supported but totally lacked in grainstones. This work depends upon the cumulative knowledge acquired through microscopic analyses of thin sections. The point counting Punktfeld -method after Sander (1951) and improved by Chayes (1956) in (Flugel, 1982) was carried out for (36) thin sections represent the whole BI. The results are shown in table 1 and 3-D Pie charts (figure 2).

Table.1: Point counting results of thin sections (Petrographic study) based on Punktfeld-method after Sander (1951) and improved by Chayes (1956) (in Flugel, 1982.

Sample No.	Mineralogical Constituents %								Calcite Components %						Iron Oxides %		
									Groundmass		Allochems						
	Calcite	Dolomite	Siderite	Phosphate	Chamosite	Glauconite	Iron oxides	Quartz	Spary	Microspar	Lithoclast	Algae	Bioclasts	Secondary Calcite (Filled veinlets)	Intergranular	Coated	Replacement
BN1/1	93.4	-	1.0	2.0	-	-	3.6	-	22.0	2.6	-	56.6	9.6	2.6	0.6	1.0	2.0
BN1/2	88.0	1.0	3.0	1.0	-	-	5.0	2.0	25.0	2.0	-	50.0	10.0	1.0	0.4	1.0	3.6
BN1/3	60.0	-	2.0	1.0	-	9	27.0	1.0	23.0	-	3.0	30.0	4.0	-	3.0	4.0	20.0
BN1/4	55.6	-	1.4	9.0	8.0	1.4	22.6	2.0	24.3	-	10.0	16.3	5.0	-	10.0	2.0	10.6
BN1/5	52.6	-	2.0	6.0	3.0	1.0	34.0	1.4	14.0	1.0	2.0	24.0	10	1.6	6.0	6.0	22.0
BN1/6	67.0	-	3.0	-	-	-	30.0	-	18.0	2.0	-	40	6	1.0	6.0	6.0	18.0
BN1/7	62.5	-	3.0	-	-	-	34.5	-	24.5	-	2.0	29.5	3.5	3.0	5.0	4.5	25.0
BN2/3	80	-	1.0	4.0	-	0.5	14.0	0.5	37	-	-	41	2	-	1	8	5
BN2/4	60	-	2.0	2.0	-	1.5	34.5	-	31.5	-	-	28.5	-	-	-	2	32.5
BN2/5	78	-	1.0	1.0	-	1.0	19.0	-	16.0	1.0	10.0	26	18.0	7	5	3	11
BN2/7	52	-	3.0	4.0	-	-	41.0	-	38.0	0.0	0.0	12	2.0	0.0		6	35
BN2/8	80	-	-	-	-	2	18		34	-	17	22	4.0	3	-	6.5	11.5
BN3/1	74	-	-	-	-	1	22	3	27	1.0	10	29	6	1	1	14	7
BN3/2	64	-	-	-	-	1	35	-	20	-	-	32	12	-	3	6	26
BN3/3	63	0.5	0.5	1	-	1	33	1	19	-	-	27	15	2.0	2.0	3.0	28
BN4/1	58	-	0.6	0.3	-	2.6	35.6	2.9	18	2	8	20	9	1.0	-	11.6	24.0
BN4/2	53	-	-	-	-	4.0	42	1.0	21	1	10	17	4	-	19	8	15
BN5/1	76.0	2.0	9.0	4.0	-	1.0	5.0	3.0	30	-	2.0	38	5	1	-	2.0	3.0
BN5/2	35	0.5	18	2.5	-	3.0	41.0	-	10	1	3.0	11	10	-	26	4	11
BN5/3	41	0.5	19.5	2	-	1.5	34	1.5	11	2.0	0.5	15	12	0.5	15	2	17
BN5/4	49	-	4.0	1.5	-	1.5	43	1.0	21	2	-	24	2	-	5.0	10.0	28.0
BN5/5	50	-	4.0	1.0	-	4.0	41.0	-	20	-	1	20	9	-	9	9	23
BN6/2	89	-	1	0.5	-	1.5	4.0	4.0	30	1	3	26	25	4.0	-	-	4.0
BN6/4	57	-	3.0	-	-	1.0	38	1.0	17	2	0.5	30	7.5	-	4	12	22
BN6/5	49	-	7.0	1.0	-	-	40	3	15	1	-	25	8.0	-	14	12	14
BN7	66	-	-	-	-	-	34	-	26	1	1	28	10	-	2	6	26
BN8/2	65.5	-	2.1	5	8.7	-	16.2	2.5	15.7	-	-	36.7	13.2	-	7.5	5	3.7
BN8/3	64.6	-	-	-	0.6	2.6	30.6	1.6	31.0	-	-	27	6.6	-	1	5	24.6
BN8/4	51	0.3	1.0	-	-	6.7	39	2	25	1	1	17	7	-	2	4	33
BN8/5	53.7	-	3.0	1.0	-	1.0	39.7	1.6	19	1.0	2.0	27	3.7	1	11.2	5.5	23.0
BN9/1	74.5	-	-	2.5	6.0	1.5	14.5	1.0	23.5	0.5	3.0	40	7.5	-	1.5	0.5	12.5
BN9/2	55	-	4	2	1	2	35	1.0	20	-	5	20	10	-	4	5	26
BN9/3	60	4	1	-	-	2.0	32	1.0	20	-	2.0	25	12	1	2	7	23
BN10/1	49	-	3	3	1	4	36	4	18	-	3	23	5	-	16	11	9
BN10/2	57.5	-	1.0	-	-	-	39.5	2.0	20.5	-	-	30	7	-	10.5	9	20
BN10/3	53	-	1.0	-	-	-	44	2.0	17.5	-	-	30	5.5	-	5.0	9	30
Max.	93.4	4	19.5	9.0	8.7	9	44	4.0	38	2.6	17	56.6	25	7	26	14	35
Min.	35	0.3	0.5	0.5	0.6	0.5	3.6	0.5	10	0	0	11	2	0	0.4	0.5	2
Av.	62.2	1.4	4.0	2.6	4.1	2.4	29.0	1.9	22.3	1.3	4.6	27.9	8.4	2.0	7.0	6.0	18.0

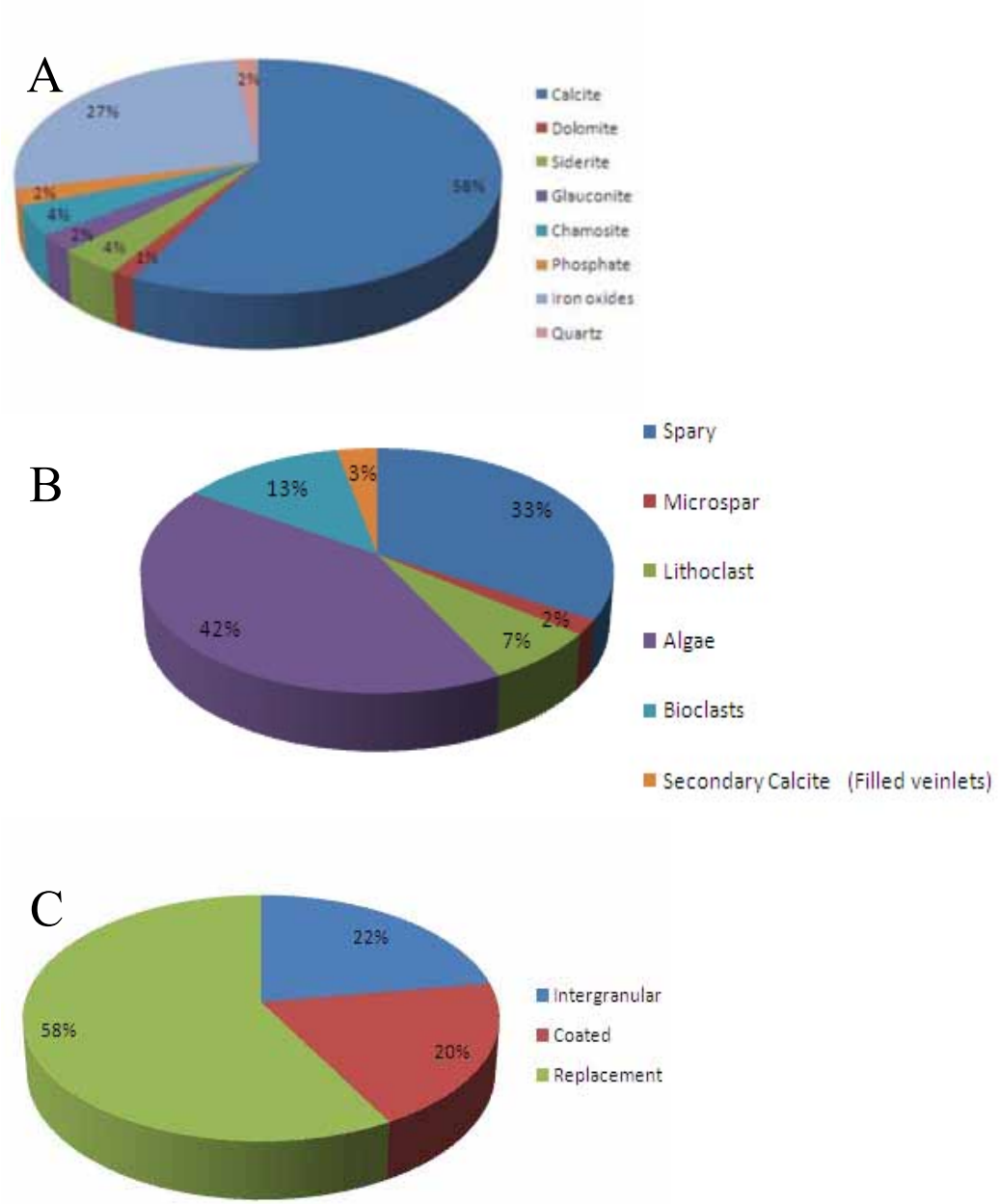

Figure 2: 3-D Pie charts based upon point counting results of BI samples showing in: A- the general mineralogical constituents, B- calcite components, and C- nature of iron oxides occurrences.

The microscopic analyses showed that the original facies of BI is an algal-bioclastic - packstone according to the aforementioned classification and the estimation by point counting results. Hallsworth and Knox (1999) mentioned that the iron rich sediments textural classification follows the textural limestone scheme. This classification scheme is summarized in table 2. Therefore, and based on above, BI is could be classified to (iron- packstone).

Table 2: The textural classification of iron- rich sediments (ironstone), after Hallsworth and Knox (1999).

Depositional texture recognisable					Depositional texture not recognisable
Contains matrix (silt and clay < 32 µm in diameter)			Lacks matrix	Components bound together by action of plants and animals in the position of growth	
Matrix-supported		Grain-supported			
> 75% matrix	< 75% matrix				
iron-mudstone	**iron-wackestone**	**iron-packstone**	**iron-grainstone**	**iron-boundstone**	**ironstone** (use qualifiers to describe crystal size)

Diagenetic processes

BI suffered from many diagenetic processes through its geological history. Replacements effects are the most common where the replacements processes have been observed in all BI samples. the following are the main types of diagenetic processes which observed in studied samples.

Iron oxides replacement

The replacement includes two processes: dissolution of an original mineral and the cavities replaced by another one (Tucker, 1981). Iron oxides replacement is the most important one among replacement processes occurred in the diagenetic history of BI. Partial replacement of fossils by iron oxides is very common (Plate 2.A).

Complete replacement is common too (Plate 2.B). Locally, iron oxides have replaced the calcareous structures produced deposits of higher than usual content. Iron oxides observed as coating of grains (Plate 2.C), filled pores (intragranular) (Plate 2.D), between grains (intergranular) (Plate 2.E), and replaces fossils especially red algae. The euhedral crystals of iron minerals (pyrite) are widely distributed in hexagonal (Plate 2.F) and cubic in shape (Plate 2.G &H). Euhedral crystals of magnetite are also present (figure 3).

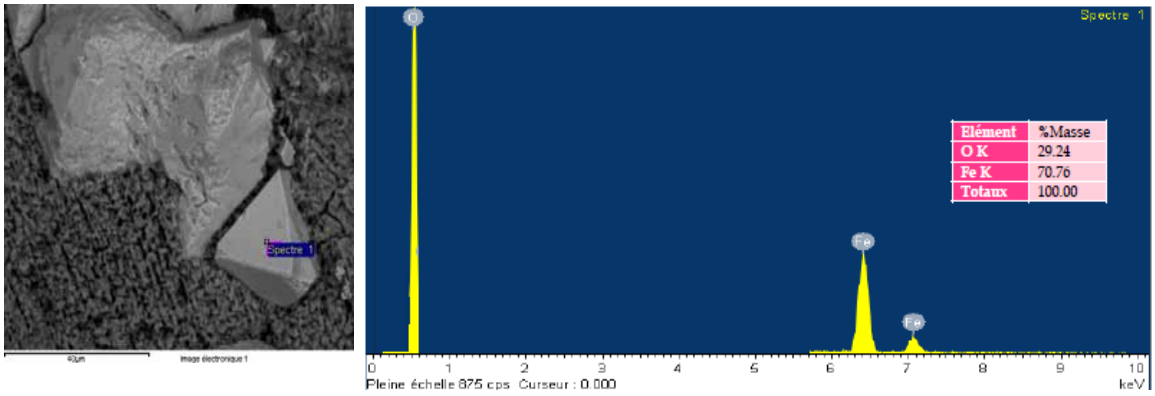

Figure 3: Backscatterd image and spectra show the euhedral magnetite crystals in BI.

Glauconitization

Glauconite occurs in very small amount at the base of BI associated with pyrite, phosphates and chamosite. The presence of glauconite indicates submarine conditions in areas of low sedimentation rate in a confined environment (Odin and Matter, 1981). The growth of glauconite inside fossils due to the prevailing of confined microenvironment is clear (Plate 3. A, B & C).

Phosphatization

Phosphate minerals are found in minor amounts. Apatite and collophane were the two phosphates mineral recognized in the studied samples. The size of apatite crystals ranges between 0.05 mm to 0.19 mm. Apatite is prominent in some iron ores (Kerr, 1959). collophane is distinguished by its massive form, which appears under plane polarized light (PPL) in light to dark brown in color, occasionally it was colorless, and by its isotropic characteristic under cross nicoles (XPL) (Kerr, 1959). Partial phosphatization of fossils is common (Plate 3.E & F) and complete replacement are observed in many samples (Plate 3-G &H), some of original phosphatic bones are also present.

Chamosite formation and sideritization

Chamosite occurs around grains which often forms the outer rim of completely or partially impregnation fossils by iron oxides, and it is distinguished by its pale green color under plane polarized light (Plate 4.A, B&C). Chamosite occurrence around fossils that are not affected by iron oxides replacement is also observed (Plate 4.D). The presence of chamosite as coating of impregnation fossils by iron oxides reveals that the paragenesis is probably; iron oxides replacement preceded chamosite formation through diagenetic history of BI. Siderite marked by interlocking rhombic grains characterized by brown stains around their borders and along cleavage cracks (Plate 4. E & F). Siderite is mostly widespread in sedimentary iron ores. The important feature of siderite is its extreme instability where it is clearly oxidized to form: goethite, hematite and other iron oxides/hydroxides minerals (Kholodov and Butuzova, 2004). Siderite also is a prominent mineral in the oolitic ironstones of England as associated with chamosite (Kerr, 1959).

Pyritization

Pyritization is quite clear in BI. Pyritization indicates anoxic or dysaerobic environments (Berner, 1970). It may be formed in diagenetic environments characterized by slow detrital addition, abundant organic matter and readily available sulfate maintain high sulfide activities (Curtis and Spears, 1968). Many experiments have shown that an oxidant is required to produce pyrite from precursor iron monosulfide where the major steps to form sedimentary pyrite are: bacterial sulfate reduction, reaction of H_2S with iron minerals to form iron monosulfide and reaction of iron monosulfide with elemental sulfur to form pyrite (Berner, 1984).

Silicification

Some bioclasts especially algae have been observed replaced by: euhedral quartz crystals that possibly authigenic in origin (Plate 5. A,B,C &D), subhedral and anhedral quartz (Plate 5.E& F), and chalcedony in part (Plate 5. G&H). The appropriate chemical conditions to dissolve calcite and precipitation of silica are supersaturated pores solutions by silica and decrease of pH and temperature. The silicification can take place during early or late diagenesis (Tucker, 1981). The source of silica probably is endogenic

from siliceous skelton debris including sponge spicules and radiolarian or the corrosion of quartz and clay minerals at high pH, when pH decreases precipitation of dissolved silica occurs; thus, this proces is produced by pH changes and decreases of temperature (Engelhardt, 1977).

Cementation

The spary calcite cement is distinguished based on calcite crystals morphology occupies the majority of the original pore space (Plate 6. A&B), this cementation was resulted from chemical precipitation of material from a solution on a free surface (Flugel, 1982).

Neomorphism

Neomorphism includes inversion and recrystallization and refers to changes of morphology, size, and orientation of calcite crystals (Folk, 1965). It is a special form of replacement where the original and new minerals have the same chemical composition. This feature is widespread in Benavi IRS and overlying country rocks (Plate 6.C and D, respectively). In some samples, pyrite crystals have been observed as floats in the groundmass of spary calcite cement. The intense effects of bioclasts by neomorphism processes probably give an interpretation for why these pyrite crystals look as floating grains (Plate 6.E, F, G&H). These photographs clarify how pyrite crystals released from the inside fossils to spary calcite. Probably, this occurred by the intense phreatic meteoric diagenesis where these plates show fossils (algae) undergone from neomorphism and also show the microstructure of algae is still visible. This leads to the possibility of arranging events as follows: Deposition fossilization, pyritization (in reduced microenvironments inside fossils), neomorphism (dissolution of calcareous fossils that recrystalized to spary calcite where pyrite crystals present inside these fossils released gradually in to spar), (Bricker, 1971).

Dolomitization and Dedolomitization

This digenetic process is very limited in BI. The presence of dolomite rhombs with silica, Plate 7. B&C, is interpreted to indicate that dolomitization preceded precipitation of silica as post depositional process (Larsen and chilingar, 1979). The dolomitization is commonly the late phase of diagenetic history (Qureshi et al, 2005). Dedolomitization was recognized in few samples (Plate 7.D). After dolomitization, the selective leaching for dolomite rhombohedron occurred and the pores partially filled by calcite druse (Evamy, 1967). This calcitization process is referred to dolomitization and predominantly takes place through contact with meteoric waters (Tucker, 1981). According to De Groot (1967) dedolomitization can only take place at or near the earth's surface. This phenomenon is one of the late digenetic processes (Dabbagh, 2006).

Compaction

There are two types of compaction clearly observed in the studied samples:

A-Mechanical compaction: evidences for mechanical compaction are represented by sutured and corroded grains margins. Fractured and dislocated grains are also noticed (Plate 7.E). B-Chemical compaction: chemical compaction and pressure dissolution of grains and sediments is a significant source of $CaCO_3$ for burial cementation. Under conditions in which the pore fluid pressure is less than the lithostatic pressure there will be a preferential dissolution of quartz or calcite grains at high stress points where they touch and precipitate quartz and calcite cement in the adjacent interstices (Flugel, 1982).

The pressure solution structure in studied samples includes the following:

1-Condenced fabric: the surface between grains vary from having point and planar (Plate 7.F), interfering to sutured and corroded grain margins (Plate 7.G), depending upon the degree of dissolution and compaction (Flugel, 1982).

2-Stylolitization: Stylolites are the zones of discontinuity within rocks. In thin section, they have undulated to zigzag sutures; the stylolite transect the grains, rock fabric, cement and matrix indiscriminately. Irregular and low peaks amplitude stylolites (Trurnit, 1968) are observed in BI and underlying country rocks samples, (Plate 7. H and I, respectively).

Discussion

The petrographical observations of thin sections have revealed the main stages of BI formation. The first stage is the deposition of bioclastic- algal - packstone under warm climate in shallow marine high energy, the fossils assemblages (algae, echinoderm …) reflects this environment (Flugel, 1982). This suggestion corresponds to that of shallow marine origin for this ore body which was suggested by Geosavod (1981). Presence of spary calcite cement also supports this opinion because a lack of micrite denotes high energy environment (Tucker, 1981). Petrographical observations indicated that dissolution of fossils preceded the precipitation of iron oxides and sometimes there is selective dissolution occurred (Selley, 2007); where these observations showed that algae affected more than other particles in the framework of the studied thin sections by dissolution and replacement processes. During early digenesis at shallow burial conditions, changes in oxidation fugacity can result in the precipitation of iron as goethite and hematite under oxidizing conditions (atmospheric effect). Probably slightly acidic solution rich in Fe^{+2} penetrated to this facies along fissures and fractures then reacted with the calcareous constituents and dissolved it partially and completely in parts where Fe^{+2} oxidized to Fe^{+3} and precipitate (Melanek,1982). Oxidation of Fe^{+2} led to release of H^{+} ; the precipitation of CaCO3 would be inhibited during periods of iron minerals formation ;otherwise these environments would be ideal for carbonates formation explaining the similarity in texture between iron formations and carbonates(Maynard, 1983). In this stage, bacteria may have played an important part in the formation of iron oxides (Stanton, 1972). The ferric oxides /hydroxides that formed in this stage are important predecessors to minerals formed later such as, magnetite that were produced during early digenesis near the sediment/water interface (Klein, 2005 in Johnson, 2008). the presence of chamosite in most BI samples contributes to understand the precisely of next stage where the formation of chamosite may have occurred after previous oxidized stage when Eh and pH changed. The reduction conditions are necessary for chamosite formation under marine conditions (Harder, 1978), an important argument for the diagenetic formation of chamosite from Fe^{+3} hydroxides in marine environment is accepted (Gartner and Schellmann, 1965 ; Porrenga, 1965 ; Rohrlich et al, 1969 in Harder, 1978). The reduction of iron in diagenetic environments followed by de-hydration (promoted by sediment compaction) would favor transformation to chamosite (Curtis and Spears, 1968), and also, chamosite may be formed from hydrated iron oxides and detrital clay minerals (especially kaolinite) during early stages of diagenesis in an iron rich environment (Karpov et al, 1976 ; Schellman, 1969 ; Bhattacharyya, 1980 ; in Bhattacharyya, 1982). Based on above and depending upon the petrographical observations that

showed chamosite occurrences around impregnation fossils by iron oxides, this does confirm chamosite growth beyond iron oxides replacement after changing of initial redox conditions in diagenetic environment. For any reason sulphide activity in the diagenetic environment was low; the reaction between organic matter and ferric components would have likely created conditions favorable for siderite formation in the presence of Fe^{+2} and carbonate activity (Curtis and Spears, 1968). Sideritization of IRH observed in many samples may be attributed to this reason. After the stage of chamosite and siderite formation and at more deep burial with conditions of intense compaction and increasing in sulphide activities, most iron components will tend to transform to pyrite (Neumann et al, 2005). The presence of pyrite throughout BI, which raised the indication of the suffering of this body with its iron content from high reduction conditions, and the more highly affected part was at the base of BI that looks dark colour in the field. Quartz, pyrite and glauconite which were observed in the BI samples are authigenic in their origin formed post-depositionally (Lisitizin, 1972), and their presence them is a good evidence for late diagenetic (Buyce and Friedman 1975 in Al-Ani, 2005). The high neomorphism effect which was identified by transformation of fossils to spary calcite, and the presence of drusy calcite texture as well as dolomitizatin, dedolomitization and silisification; probably represent the late stage of diagenetic history occurred beyond the uplift of BI and country rocks above sea level, as conditions of phreatic & vadoze zone were prevailing, respectively (Longman, 1980). The transformation of: (pyrite, siderite and chamosite) to: (goethite, limonite and hematite), as well as, dehydration of goethite to form hematite may be belong to this stage with its effects going on.

Conclusions

Petrographical study of BI demonstrates the following conclusions:

1. BI is related to algal-bioclastic-packstone host rocks which suffered from many diagenetic processes such as: iron oxides replacements, phosphatization, pyritization, neomorphism, silicification, cementation, and goethitization, in adition to mechanichal and chemical compaction, with limited processes of dolomitization & dedolomitization.
2. Chamosite mostly occurs around impregnation fossils by iron oxides, this does confirm that chamosite growth is beyond iron oxides replacement after changing in initial redox conditions in diagenetic environment**.**
3. Quartz, pyrite and glauconite are authigenic in their origin formed post-depositionally and their presence is a good evidence for late diagenetic.

The high neomorphism effect that converted the fossils to spary calcite, and the presence of dolomitizatin, dedolomitization and silicification; occurred beyond the exposure of BI and country rocks above sea level, as conditions of phreatic & vadoze zone were prevailing, respectively; the transformation of: (pyrite, siderite and chamosite) to: (goethite, limonite and hematite), as well as, dehydration of goethite to form hematite may be belong to the late stage of diagenetic history.

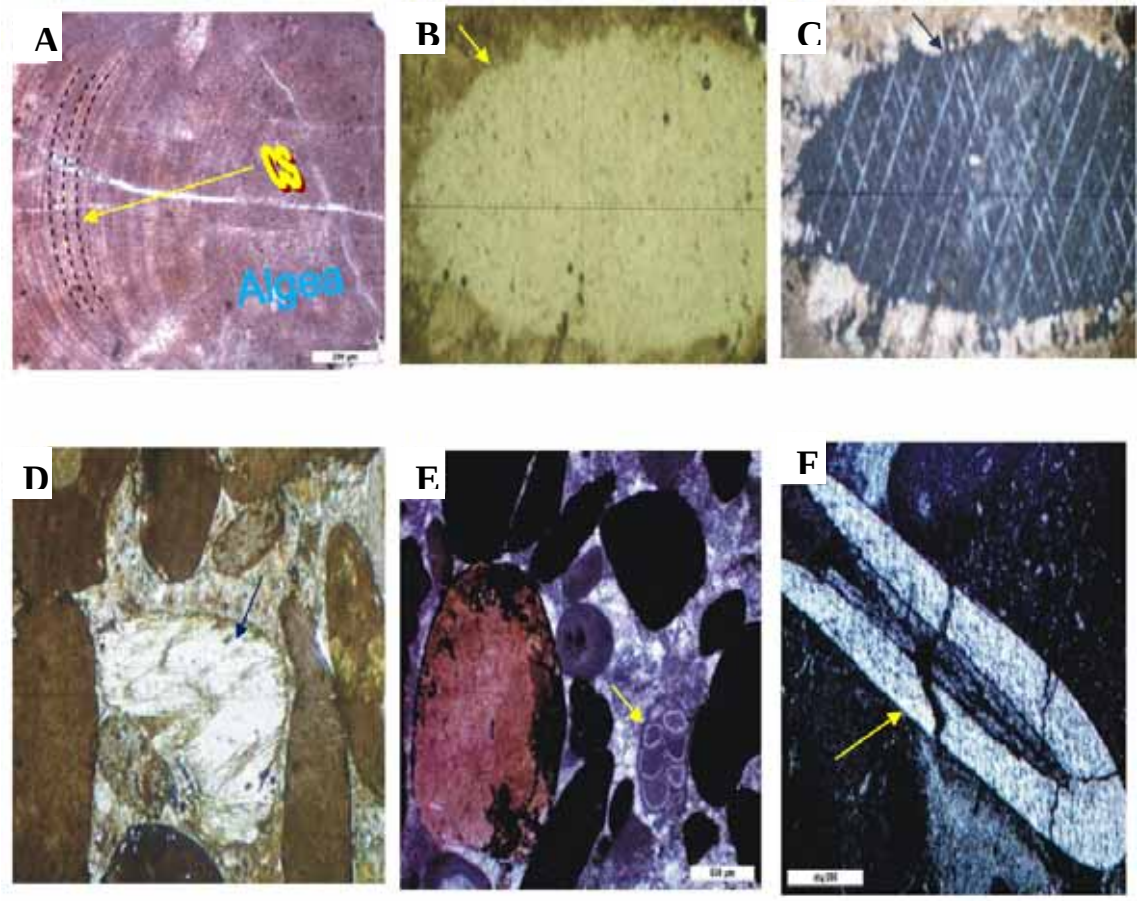

Plate 1: Photomicrographs show: A. calcareous red algae with it's fine cellular structure (cs), sample no. (BN2/3), (20X), PPL. B. presence of echinoderm in BI, sample no. (BN4/3), (20X), PPL. C. the same of previous showing the optical behavior of echinoderm as a single crystal of calcite, (20X), XPL. D. Shell fragment, sample no. (BN5/3), (20X), PPL. E. Biserial Foraminifera, sample no. (BN6/2), (10X), PPL. F. Sponge specules, sample no. (BN6/4), reflected light, PPL.

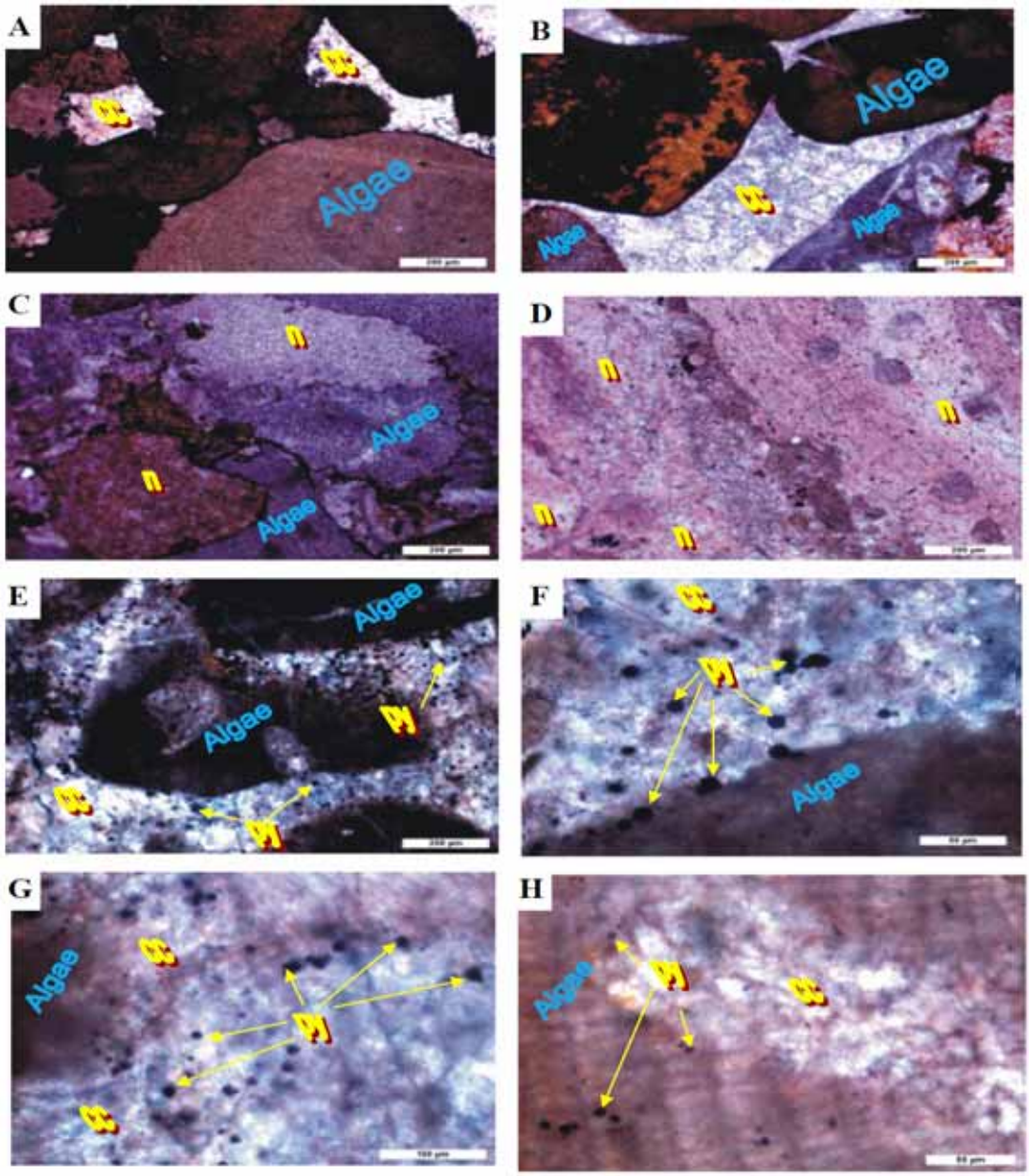

Plate 2: Photomicrographs show: A. partially replacement (pr) of fossils (Algae), by iron oxides, sample no. (BN6/3), (5X), PPL. B.completely replacement (cr) of fossils (Algae) by iron oxides, sample no. (BN2/5), PPL. C.iron oxides occurrence as coated (cd) of grains, sample no.(BN4/1),PPL. D.iron oxides occurrence as filled of pores inside fossils (intragranular), sample no. (BN2/7), PPL. E.iron oxides occurrence filled pores between grains (intergranular), sample no. (BN6/5), PPL. F.iron minerals as hexagonal euhedral crystals, sample no. (BN1/5), PPL. G.iron minerals as cubic euhedral crystals, sample no. (BN1/5), PPL. H. iron minerals as twin cubic euhedral crystals, sample no. (BN5/5), (40X), PPL.

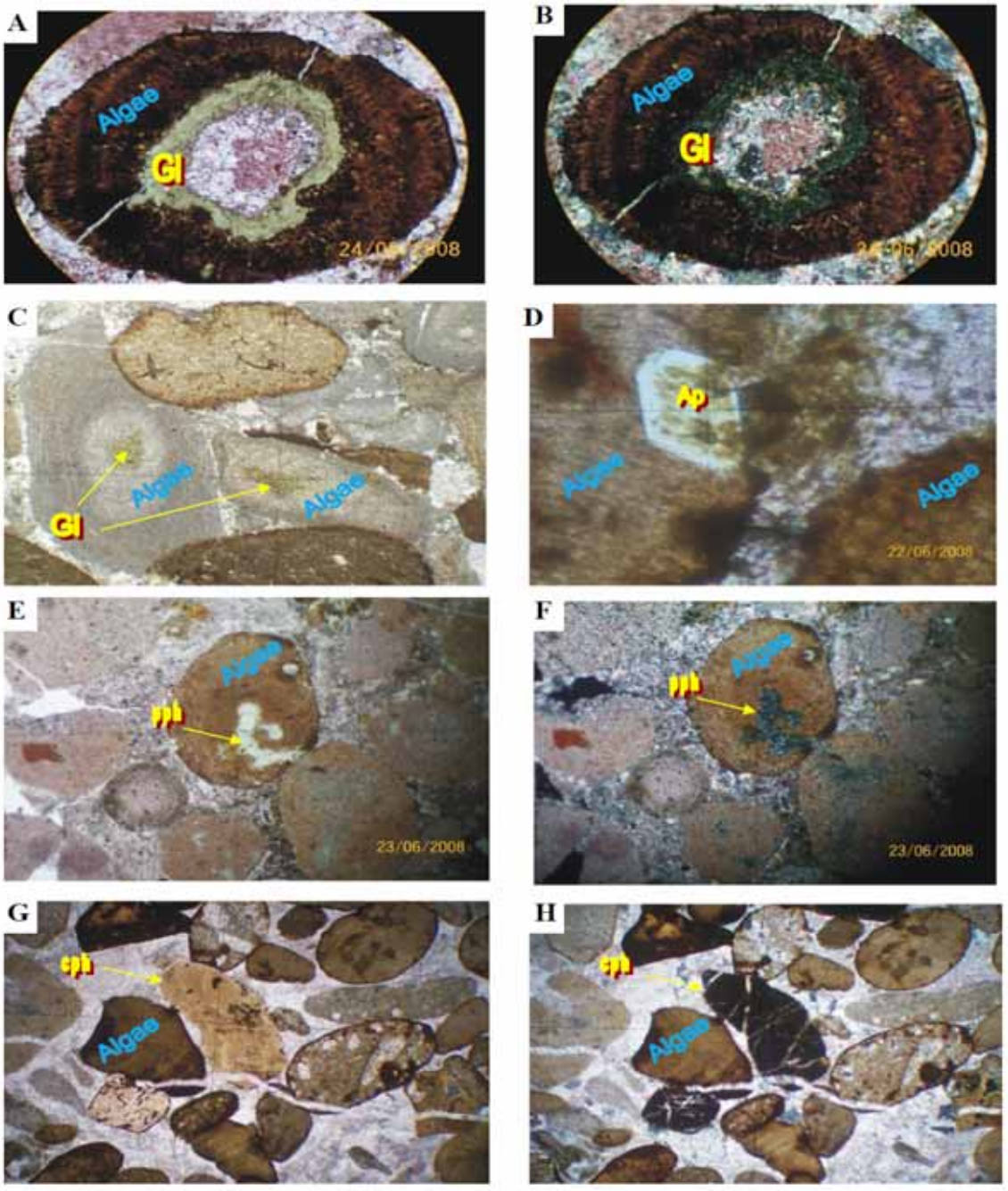

Plate 3: Photomicrographs show: A. glauconite(Gl) inside fossils (Algae), sample no. (BN9/1), (20X), PPL. B. The same as previous but under XPL. C. glauconite (Gl) inside fossils (Algae), sample no. (BN8/3), (10X), PPL. D. six-sided prismatic crystal of apatite (Ap), sample no. (BN3/1), (20X), PPL. E. partial phosphatization (pph) of fossils (Algae), sample no. (BN3/1), (10X), PPL. F. The same as previous but under XPL. G. complete phosphatisation (cph), of fossils (Algae), sample no. (BN8/4), (5X), PPL. H. The same as prevoius but under XPL.

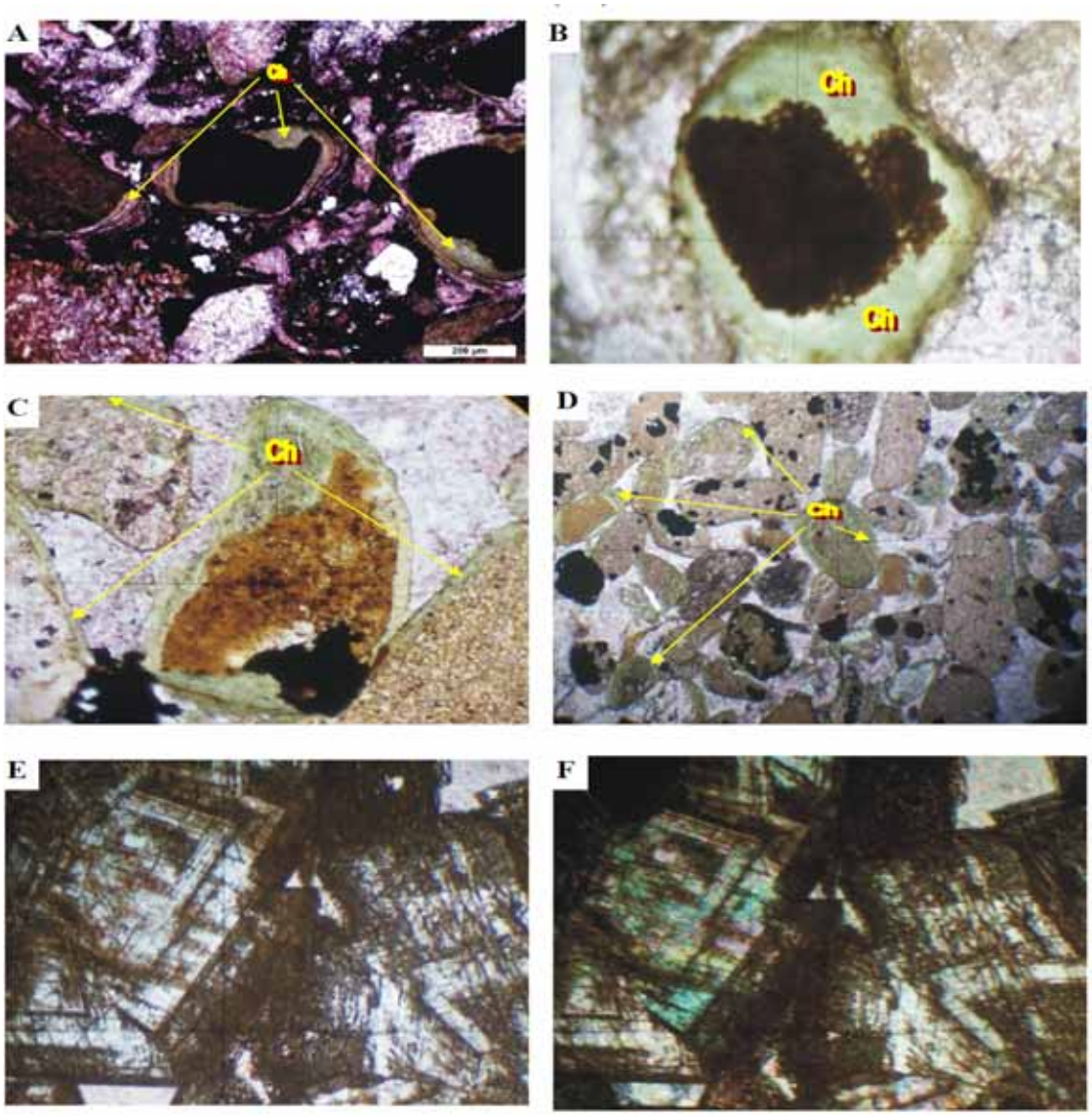

Plate 4: Photomicrographs show: A.chamosite (ch) as outer rim of completely impregnated fossils by iron oxides, sample no. (BN1/4), PPL. B. chamosite (ch) as outer rim of completely impregnated fossils by iron oxides, sample no. (BN9/1), (20X), PPL. C. chamosite (ch) as outer rim of partially impregnated fossils by iron oxides, sample no. (BN8/2), (20X), PPL. D. chamosite (ch) around fossils not affected by iron oxides replacement, sample no. (BN2/3), (5X), PPL. E. siderite rhomb grains and the brown stains along cleavage, sample no (BN5/2), (40X), PPL. F. The same as previous but under XPL.

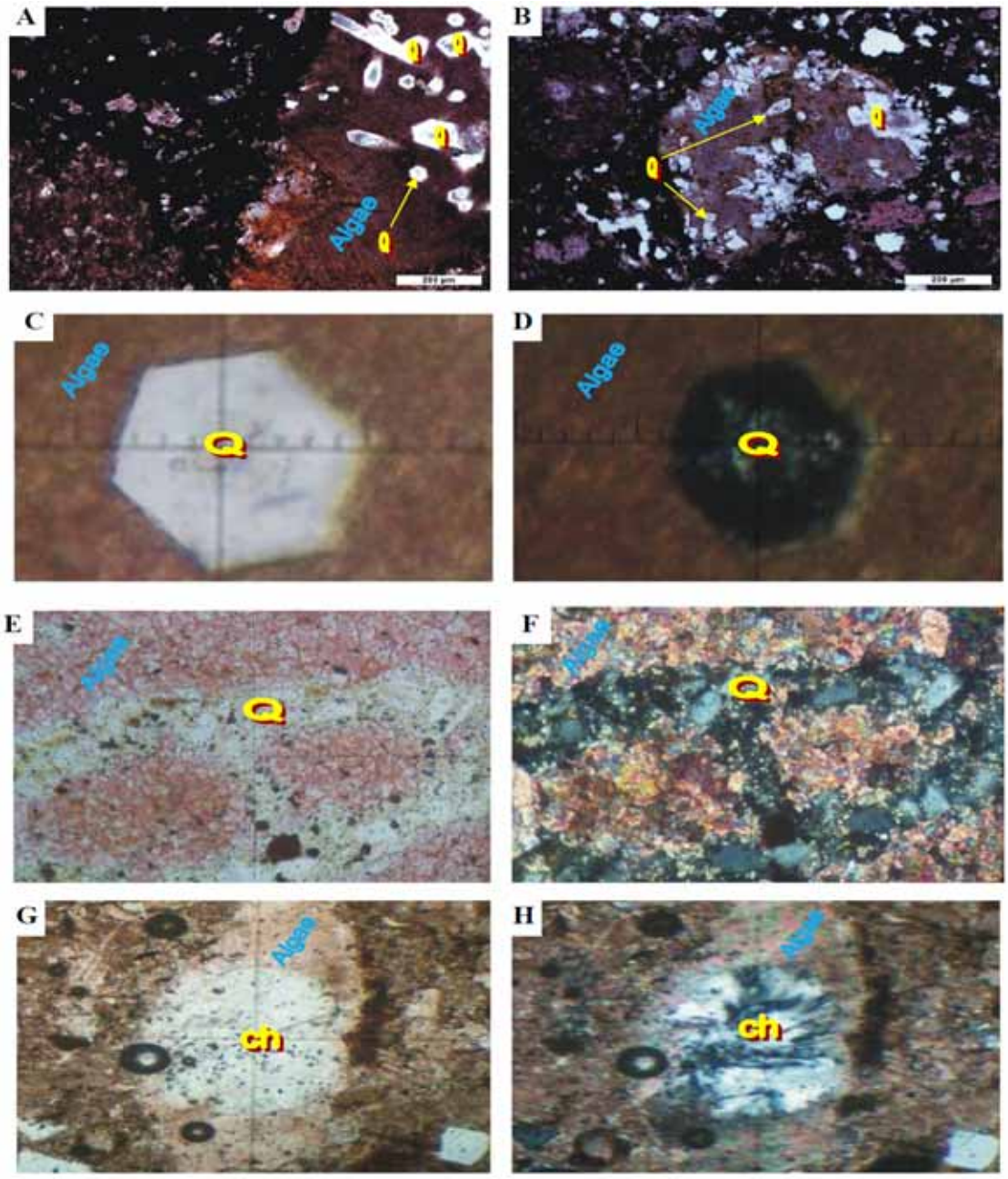

Plate 5: Photomicrographs show: A. euhedral quartz (Q) replaced parts of fossils (Algae), sample no. (BN1/2), PPL. B. euhedral quartz (Q) replaced parts of fossils (algae), sample no.(BN6/2),PPL. C. euhedral quartz(Q) replaced parts of fossils (Algae), sample no.(BN10/1),PPL. D. the same as previous but under XPL. E. anhedral quartz (Q) replaced parts of fossils (Algae), sample no.(BN3/1), (40x), PPL. F. As the same of previous but under XPL. G. chalcedony (ch) replaced parts of fossils (Algae), sample no. (BN4/1), (40x), PPL. H. the same of previous but under XPL.

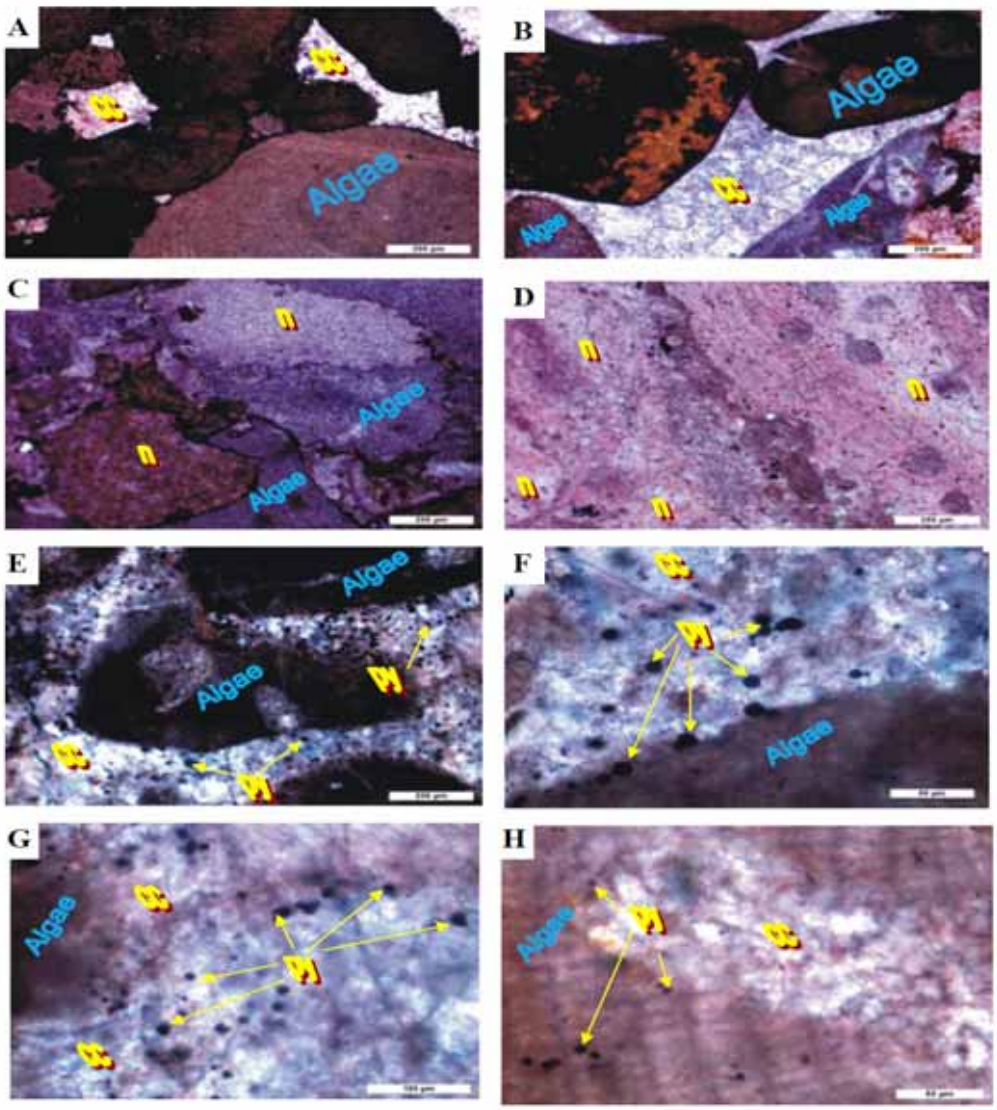

Plate 6: Photomicrographs show: A. spary calcite cement (cc) filled pore spaces between grains sample no. (BN5/5), PPL. B. spary calcite cement (cc) filled pore spaces between grains, sample no. (BN1/3), PPL. C. the neomorphism(n) feature, sample no. (BN10/2), PPL. D. the highly neomorphism (n) in overlying country rocks of IRS, sample no. (BN1/8). E. pyrite (py) crystals float in spary calcite cement (cc), sample no. (BN5/2), PPL. F. pyrite (py) crystals released from skeletal of fossils(Algae) to spary calcite cement(cc) by the effect of neomorphism, higher magnification than previous Plate, (BN5/2), PPL. G. As the same of previous in another site, sample no. (BN5/2), PPL. H. pyrite (py) crystals released from inside fossils(Algae) to spary calcite cement (cc) by the effect of neomorphism, high magnification, sample no. (BN6/4).

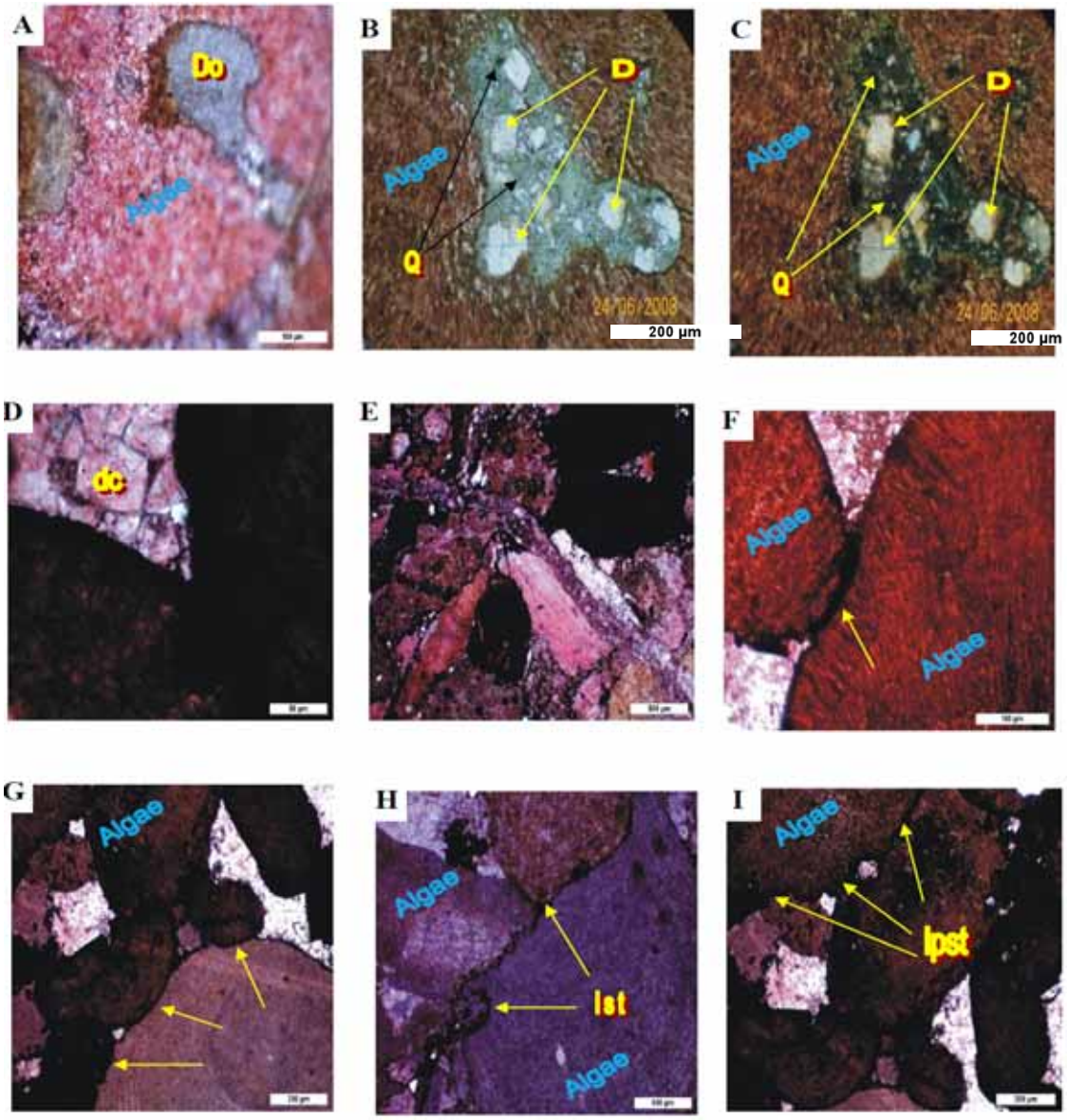

Plate 7: Photomicrographs show: A. the dolomitization (Do) feature, sample no. (BN5/1), (20X), PPL. B. rhombs of dolomite (D) crystals associated with quartz, sample no. (BN10/1), PPL. C. the same of previous, XPL. D. dedolomitized calcite (dc) cement due to dedolomitization phenomenon, sample no. (BN9/1), PPL. E. the mechanical compaction feature, sample no. (BN2/7), PPL. F. the surface contact between grains which vary from point and planar, sample no. (BN4/1), PPL. G. the sutured and corroded grain margins due to compaction and dissolution, sample no. (BN6/4), PPL. H.irregular stylolite (ist) phenomenon in BI, sample no. (BN4/2), PPL. I. low peaks amplitude stylolite (lpst) phenomenon in BI samples, sample no. (BN7), PPL.

References

Al-Bassam, K., 1972, Reconnaissance mineralogical study of some lead –zinc deposits in northern and northeastern Iraq, Unpubl. M.Sc. Thesis, University of Wales, U.K., 55p.

Ali,A.A,2007, Sedimentology of Shiranish formation in selected areas from Northern Iraq, Unpubl.Ph.D.Thesis. Baghdad university,220p.

Babalola,L.O., Hussain,M. and Hariri,M.M.,2003, Origin of iron- rich beds in the basal Wajid sandstone, Abha-Khamis Mushayt area, Southwest Saudi Arabia, The Arabian J. for science and Engineering, V.28,no.1A,pp 3-24.

Bellen,R.C. Dunnigton, H.V.,Wetzel,R., and Morton,D.,1959, Lexique stratigraphic Internat. Asie, Fasc.10, Iraq, Central national deal Recherches Scientifique,Paris,333p.

Berner,R.A.,1970, Sedimentary pyrite formation, Am.J.Sci.V.268, pp1-23.

Berner,R.A.,1984, Sedimentary pyrite formation :An update, Geochim. Cosmochim. Acta.,V.48, pp605-615.

Bhattacharrya, D.P., and Kakimoto,K.P.,1982, Origin of ferriferous ooids, an SEM study of ironstones ooids and Bauxite pisoids, J. Sed. Petrol.,V.52,no.3,pp849-857.

Boukhtoyarov, I.S. and Yevlentyev, I.V., 1962, On 1:200000 prospecting correlation of the area between the Greater Zab and Khabour Rivers, GEOSURV, Baghdad, Rep. no. 291, 36p.

Bricker, O.P.,1971, Carbonate cements, Jhon Hopkins Press. Ltd., London, 376p.

Buday, T. and Vanecek, M., 1971, Outlines of mineral occurrences of Iraq and general mineral investigation program for 1971-1990, GEOSURV, int. rep. no. 509.

Buday, T., 1980, The regional geology of Iraq, Stratigraphy and Paleogeography, Kassab, I.I. and Jassim, S.Z., (eds), Dar Al-Kutib Publ. House, Mosul, Iraq, 445p.

Buyce, M.R., and Friedman, G.M., 1975, Significant of authiginic Kfeldspar in Cambrian Ordivician carbonate rocks of the proto-atlantic shelf in north America, J.Sed.Petrol.,V.45, pp808-821.

Chaickin, S.I., 1970, Report on the iron ore potentialities in Iraq and recommendation on the trend of further geological iron ore exploration ,GEOSURV, int. rep. no. 548.

Craig, J.R., Vaughan, D.J., 1981, Ore microscopy and ore petrology, Jhon Wiley & Sons.Inc., U.S.A., 406pp.

Crerar, H.D., Namson, M.S., Chyi, L., and Feigenson ,M.D. ,1982, Manganiferous cherts of the Franciscan assemblage ,general geology, ancient and modern analogues and implications for hydrothermal convection at oceanic spreading centers, Econ.Geol., V.77, pp519-540.

Curtis, C.D., and Spears, D.A., 1968, The formation of sedimentary iron minerals, Econ. Geol., V. 63, pp262-270.

Dabbagh, M.E., 2006, Diagenesis of Jurassic Tuwaiq mountain limestone central Saudi Arabia , J.king saud.univ.,Riyadh, V.19, pp31-58.

De Groot,K., 1967, Expermental de dolomitization texture, J. Sed. Petrol., V 37, pp1216-1220.

Dickson, J.A.D., 1965, A modified staining technique for carbonates in thin section, Nature, V.205, no.4971, p.587.

Dunham, R.J., 1962, Classification of carbonate rocks according to depositional texture. In Ham, W.E., (ed), classification of carbonate rocks, A symposium Am. Ass. Petrol. geologists, Memior 1, Talusa , Oklohoma, U.S.A, pp108-121.

Embry, A.F., and Klovan, J.E., 1971, A late Devonian reef tract on northeastern Banks Island,Northwest Territories, Bull. Can. Petrol. Geol.V.19, pp730-781.

Engelhardt, W.V., 1977, The origin of sediments and sedimentary rocks, E. Schweizer bursche Verlag sbuch handing (Nagela U.ober miller), Stuttgart, 359p.

Etabi, W., 1982, Iron ore deposits and occurrences of Iraq, GEOSURV, int. rep. no. 1324.

Evamy, B.D., 1967, Dedolomitization and the evelopment of rhombohedral pores in limestones, J.Sed.Petrol., V.37, 1204-1215.

Folk, R.L., 1965, Some aspects of recrystalization in ancient limestone, In: Pray, L.C., and Murray, R.C., (EDs.), Dolomitization and limestone diagenesis, Spec. Publ. Soc. econ. Paleont. Miner. 13, Talusa, pp14-48.

Flugel, E., 1982, Microfacies analysis of limestone, Springer-Verlag, Berlin, 633p.

Frederic, D., Mullet, M., Bernard, H., and Michot, L., 2005, Pyrite oxidation by hexavalent chromium :solution species and surface chemistry, Environmental Science Technology, V.39, pp 8747-8751.

Friedman, G.M., 1959, Identification of carbonate minerals by staining methods, J. sed. Petrol., V.29, pp 87-97.

Gartner Von, H.R., and Schellmann, W., 1965, Rezente sedimente in Kustenbreich der Halbinsel Kaloum ,Guinea, Mineral. Petrogr. Mitt.10, pp 349-367.

Geozavod (Yougoslavia), 1981, Geological investigation in Duri-Serguza lead-zinc deposit, N. Iraq , GEOSURV, int. rep. no. 1145.

Hallsworth, C.R. and Knox, O.B., 1999, Classification of sediments and sedimentary rocks, British geology survey, U.K., research report number 99-03, 44p.

Harder, H., 1978, Synthesis of layer silicate minerals under natural conditions, J. of clay and clay minerals, V.26, no.1, pp65-72.

James, H.L., 1966, Chemistry of the iron – rich sedimentary rocks , U.S. Geol. Surv. Prof. Paper 440W, pp47-60.

Karpov, P.A., Losev, A.L. and Shilin, A.V., 1967, Mineralogy and conditions of devonian oolitic iron ores formation on the eastern slope of voroneze ateclise, Lithology and mineral recources, pp321-330.

Klein, C., 2005, Some Precambrian Banded Iron Formations (BIFS) from around the world, their age ,geologic setting, mineralogy, geochemistry and origin, Am. Mineral, V.90, no10, pp1473-4990.

Kerr, P.F., 1959, Optical mineralogy, (3rd Ed.), Mc Graw-Hill, N. Y., 442p.

Kholodov, V.N., and Butuzova, G.Y., 2004, Problems of siderite formation and iron ore Epochs, Lithology and Mineral Recources, V. 39, no.5, pp389-411.

Larsen, G. and Chilingar, G.V., 1979, Diagenesis in sediments and sedimentary rocks, Elsevier, Amsterdam. 579p.

Listizin, A.P., 1972, Sedimentation in the world ocean, Spec. Publ. econ. Paleont. Miner. Tulsa, 218p.

Longman, M.W., 1980, Carbonate diagenesis textures from nearsurface diagenetic environments, Bull. Am. Ass. Petrol. Geol., V.64, pp461-487.

Maynard, J.B. 1983, Geochemistry of sedimentary ore deposits, Springer-Verlag, N. Y., 305p.

McCarthy, M.J., 1955, Final report on geology between the Zab and Khabour rivers, north of Amadia, GEOSURV, int. rep. no. 266.

Melnik, Y.P., 1982, Precambrian banded iron formations, Elsevier Scientific Publishing Co.Amsterdam, 310p.

Neumann, T., Rausch, N., Leipe, T., Dellwig, O., Berner, Z., and Bottcher, M.E., 2005, Intense pyrite formation under low-sulfate conditions in the Achterwasser lagoon, SW Baltic sea, Geochim.et Cosmochim. Acta.,V.69, no.14, pp3619-3630.

Newman, D.K., and Kappler, A., 2004, Formation of Fe III minerals by Fe II-Oxidizing photoautotrophic bacteria, Geochim. et Cosmochim. Acta. ,V.68, no.6, pp 1217-1226.

Odin, G.S., and Matter, A., 1981, Glauconite origin. Sedimentalogy, V. 28 , pp 611 - 641.

Rohrlich, V., Price, N.B., and Galvert, S.C., 1969, Chamosite in the recent sediments of Loch Etive , Scotland. J. Sed. Petrol., V. 39, pp 624-631.

Ostrom, M.E., 1961, Separation of clay minerals from carbonate rocks by using acid, J. of sed. Petrol. ,V.31. pp123-129.

Pettijohn, F.J., 1975, Sedimentary rocks, Harper &Row, N. Y., 628p.

Porrenga, D.H., 1967, Glauconite and chamosite as depth indicators in the marine environment, Mar. Geol., V.5, pp 495-501.

Qureshi, M.K., Masood, K.R. and Butt, G.A., 2005, Lithofacies analysis of the lower cretaceous Lumshiwal formation,Kalla Chitta Range, northern Pakistan, Geol. Bull. Punjab. univ., V.40, pp 1-19.

Schellman, W., 1969, Sedimentalogy chamosite and hematite , News Jahrb. Min. Geol. Pal. Abh., V.111, pp1-31.

Selley, R.C., 2007, Applied Sedimentalogy, (2 nd. Ed.). Academic Press. USA. 543p.

Stanton, R.L., 1972, Ore petrology, Mc Graw-Hill Book, U.S.A, 713 p.

Taylor, J.H. 1949, Petrology of the Northampton Sand Ironstone Formation, Mem. Geol. Surv. U.K., 111p.

Trurnit, P., 1968, Presure solution phenomenon in detrital rocks, Sed. Geol., Amsterdam, V.2, pp89-114.

Tucker, M.E., 1981, Sedimentary petrology, an introduction, Blackwell Scientific Publications, Oxford, 252p.

Wetzel, R., 1950, Stratigraphic of the Amadia region, MPC report, NIMCO Library. no. TR/RW12, Baghdad.

Wilkin, R.T. and Barnes, H.L., 1997, Formation processes of framboidal pyrite, Geochimica cosmochimica Acta, V.61, no.2, pp323-339.

Yassin, A. T., 2009, Mineralgy, petrography and geochemistry of iron rich sediments in Benavi Area Northern Iraq, Unpubl. M.Sc. thesis, Baghdad University, pp.150.

Yassin, AT and Mahmoud, MM, 2012, Mineralogy of iron-rich sediments of Benavi Area in Kurdistan Region - Northern Iraq. In: Broekmans, MATM (editor): Proceedings of the 10th International Congress for Applied Mineralogy (ICAM), Trondheim, Norway: 781-788.

Young, T.P., and Taylor, W.E., 1989, Phanerozoic ironstones, an introduction, Geological Sociaty Special publication no. 46, pp ix-xxv.